

## Rolling-Ball Viscometer for Studying Water and Aqueous Solutions under High Pressure

Seiji Sawamura and Takashi Yamashita

Department of Applied Chemistry, Ritsumeikan University, Kusatsu, Shiga, 525-8577, Japan  
E-mail: sawamura@se.ritsumei.ac.jp

A high-pressure rolling-ball viscometer designed by us about 14 years ago has been improved in some parts such as a ball, a detector, etc. and become simpler in operation and more reliable. It is possible to estimate the instrument constant at high pressures without any standard viscosity data of water at the pressures for the calibration. The high-pressure viscosity of water itself has been measured by using our viscometer. The results for H<sub>2</sub>O and D<sub>2</sub>O are shown in the region of 0.10-350 MPa and 253-298 K, including the method of calibration of the viscometer at high pressures.

### 1. Introduction

We have designed a high-pressure rolling-ball viscometer about 14 years ago [1]. It is a corrosion-resistant type and allows us to measure aqueous electrolyte solutions [2-8] and to make the whole system compact; (1) only one detector is used and (2) an oil separator is directly connected to the viscometer tube inside the pressure vessel. Calibration of the high-pressure viscometer using standard data of the viscosity at high pressures, usually those of pure water, has been troublesome and restricted the region of pressure and temperature in the measurements.

We have improved the viscometer in some parts; a ball, a detector, etc., and enhanced the simplicity in the measurements and the reliability of the viscosity. And finally, it has been possible to estimate the instrument constant at high pressures without any high-pressure data of the viscosity. This means that the viscosity at high pressures where standard viscosity is unknown can be measured by using our viscometer.

In the present work, the detail of our viscometer are described and the observed viscosities of H<sub>2</sub>O and D<sub>2</sub>O at the pressures, 0.10-350 MPa, and temperatures, 253-298 K are shown.

### 2. Experimental

**2.1. Sample** A sample of H<sub>2</sub>O was distilled with a trace of potassium permanganate after deionized. D<sub>2</sub>O (> 99.90%) was purchased from EURISO-TOP and used without any purification. These samples were filtrated with a membrane filter (pore

size 0.1  $\mu$  m) before use. Organic solvents (Nacalai Tesque Co.) were used without further purification.

**2.2. Pressure Vessel and Inner cell** Pressure vessel and inner cell are shown in Fig. 1. The inner cell consists of a viscometer tube, a ball, and an oil separator. The viscometer tube and the ball are made of Pyrex 7740 glass and other parts of the inner cell, that is, connectors and O-rings are made of fluoride resin and rubber, respectively. Therefore the cell can be used to corrosive samples such as electrolyte solution. Bore size of the viscometer tube (A) was precisely made as follows: the glass tube was melted at a high temperature around a metal rod which was precisely machined and cooled down, and then the rod was pulled out changing the temperature. The ball (B) for our initial viscometer [1] was made by polishing one by one, and the roundness attained to at most 3  $\mu$  m. It is not enough in accuracy and not easy in making. Then a new method was cited, which was the same one as making bearing steel balls. It was applied to Pyrex 7740 glass (the same material of the viscometer tube). And the balls whose roundness were better than 0.2  $\mu$  m (diameter 8.00 mm) were selected from many ground balls. The roundness was measured with a machine of Talyrond 73 type (Taylor Hobson). An oil separator (F) and a piston are used to separate a hydraulic oil from a sample solution in the inner cell and is made by cutting a hard-glass hypodermic syringe. Volume of the inner cell can be reduced with the piston in

the separator by smoothly moving when the pressure is applied.

A pair of sapphire windows (I) is attached to the pressure vessel and a light beam which comes from outside of the vessel through the optical fiber goes through the window and then the inner cell. A pair of orifices (1 mm inner diameter and 10 mm length, not shown in Fig. 1) is inserted to the window plugs (J) to cut dispersed light. The viscosity of the sample solution is estimated from the time when the rolling ball interrupts the light beam.

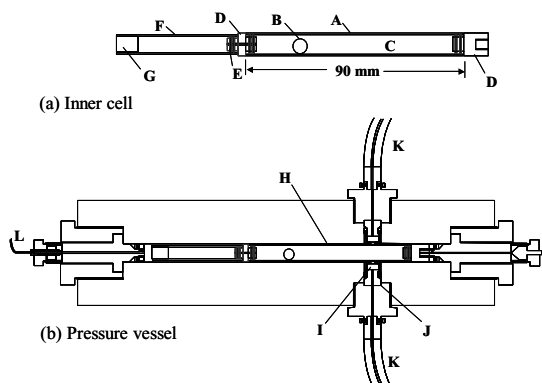


Fig. 1. Inner cell (a) and pressure vessel (b).

A: viscometer tube, B: ball, C: sample, D: connector, E: o-ring, F: oil separator, G: piston, H: inner cell, I: sapphire window, J: plug, K: optical fiber, L: pressure tube.

### 2.3. Whole System of the High-Pressure Viscometer

Whole system of the high-pressure viscometer is shown in Fig. 2. The viscometer (B) is placed on a seesaw and immersed in a water bath regulated within  $\pm 0.01$  K. The viscometer is declined and fixed at a constant angle ( $\theta$ ) by pushing it on a block (C) when the viscosity is measured. In the previous viscometer, a light-emitting diode and a phototransistor which were directly attached to each window in the water bath were used as a light source and a light detector, respectively. They were connected electric wires leading to an electric power and amplifier outside of the water bath. But in this system the measurement could not be continued for a long term because some leaking of water was caused at the light source and detector in the water bath. Then in the present viscometer, we have applied a pair of optical fibers to the system and the light

source (a 50 watt halogen lamp and a current-regulated electric power (Takasago GMO18-5.5, using a condition of DC 4A and 10 V)) and a light detector (a photodiode type (Matsusada Precision Inc., AMP-R311FC)) were placed in the outside of the water bath. In this system, any trouble of water leaking was avoided.

Hydraulic pump (Hikari High-Pressure Machinery Co., KB-10, max 1000 MPa) and a precise Bourdon gauge (Dresser Industries, Heise, max 700 MPa and 0.5 MPa/digit) are connected to the viscometer with 1/16 inch-diameter flexible tube (SUS 316).

It is important precisely to regulate the temperature because the viscosity depends on temperature. In some cases, temperature of a pressure vessel has been regulated using a metal jacket into which temperature-regulated water is circulated. But in such system, the regulation is incomplete because some parts of the pressure vessel are exposed to atmosphere. Then, in the present work, we immersed the viscometer in a water bath.

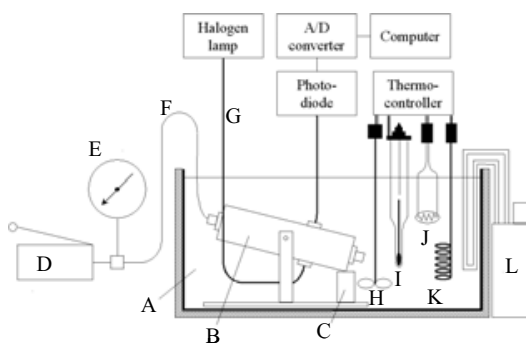


Fig. 2. Whole system of the high-pressure viscometer. A: water bath, B: pressure vessel with a seesaw, C: block, D: hydraulic pump, E: pressure gauge, F: 1/16-inch tube, G: optical fiber, H: stirrer, I: thermosensor, J: heater, K: cooler, L: auxiliary cooler unit.

## 3. Result

**3.1. Measurement of Rolling Time** When the ball rolls by declining the viscometer tube, a time course of the voltage which is detected at the optical detector is observed as shown in Fig. 3. The voltage falls to zero when the ball blocks the light beam. Anomaly high-voltage peak at the middle position in Fig. 3 is ascribed to the ball at the center

of the light beam; the transparent ball serves to focus the light beam as a convex lens. The rolling time,  $t$ , was estimated to be a period between the times at a half-voltage change as shown in Fig. 3.

The time  $t$  was measured initially at atmospheric pressure and then done at next pressures. Sometimes the pressure was returned to atmospheric pressure and the reproducibility of the  $t$  value was checked. In the measurement at lower temperatures than 273.15 K for H<sub>2</sub>O (and 276.9 K for D<sub>2</sub>O), the temperature at atmospheric pressure is placed as the reference condition and the measurement was proceeded to a high pressure and low temperature region avoiding any freezing and then returned to the reference condition. It took at least one or two hours for an equilibration at each measurement point. The reproducibility of  $t$  was  $\pm 0.15\%$ .

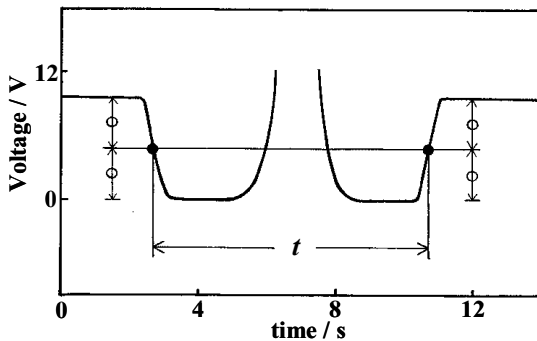


Fig. 3. A typical time course of the voltage in the detector. Sample is H<sub>2</sub>O at 273.15 K and 0.10 MPa.

**3.2. Estimation of the Viscosity** Equations (1) and (2) are generally used to estimate the viscosity,  $\eta$ , from the measurement using a rolling-ball viscometer [9, 10];

$$\eta = K(\rho_b - \rho) t \tag{1}$$

$$K = 0.0333g (\sin \theta) d(d + D) \times [(D - d)/D]^{5/2} / l, \tag{2}$$

where  $K$  is an instrument constant,  $\rho_b$  density of the ball,  $\rho$  density of a sample liquid,  $g$  the gravity acceleration,  $\theta$  declined angle of the viscometer tube,  $d$  diameter of the ball,  $D$  inner diameter of viscometer tube,  $l$  rolling distance of the ball (taken as the same as  $d$ ). As  $K$  might change on each filling of the sample liquid in the inner cell, we

estimated the ratio of viscosity as shown in eq. (3) and then the  $\eta$  was estimated using a known  $\eta_0$  value.

$$\eta / \eta_0 = K/K_0 [(\rho_b - \rho) / (\rho_{b0} - \rho_0)] (t/t_0), \tag{3}$$

where subscript 0 means the reference condition (usually atmospheric pressure at each temperature).

**3.3 Condition of the Rolling-Ball Viscometer**

*Pre-rolling distance* : Figure 4 [11] shows a relation between  $t$  and a pre-rolling distance,  $x$ , before the ball arriving at the light beam. It was performed by changing the starting position of the ball by inserting a rod of fluoride resin to the viscometer tube. This figure shows that the ball attained to a terminal velocity after a pre-rolling distance of 15 mm. Usual pre-rolling distance of our viscometer is 36 mm which is long enough to attain to the terminal velocity.

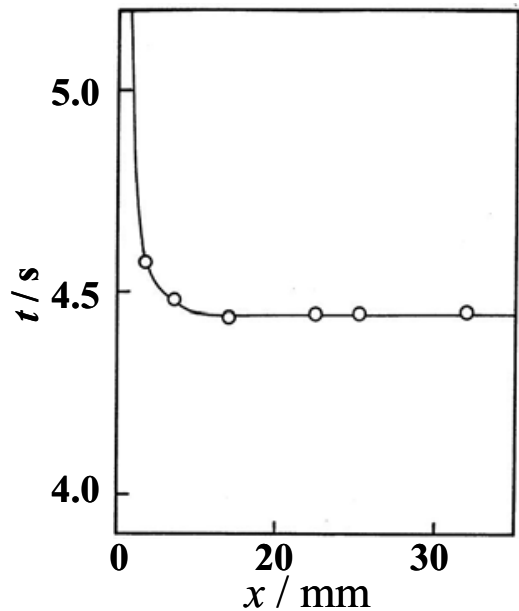


Fig. 4. Rolling time ( $t$ ) and pre-rolling distance ( $x$ ). Sample is H<sub>2</sub>O at 298 K, 0.10 MPa, and  $\theta=10^\circ$  [11].

*Rolling or Slipping of the Ball* : In using a rolling ball viscometer, it is important whether the ball is rolling or slipping in the viscometer tube. As our tube is made of transparent glass, we can observed the condition of the ball in the declined viscometer

tube outside the pressure vessel, using a microscope. Then we confirmed that the ball rolled without any slipping even at  $\theta = 30^\circ$  (at more high angle, we could not see the condition because of a too-fast moving). The declined angle in our measurement is at  $10^\circ$ .

*Condition for Laminar Flow:* In Fig. 5, the value of  $\eta / [(\rho_b - \rho)t]$  for H<sub>2</sub>O was plotted as a function of  $\sin \theta$  changing the inner diameter of the viscometer tube and declined angle at atmospheric pressure. Dotted line is a critical Reynolds number estimated by Hubberd and Brown [9]. Under this dotted line, observed values are well fit to each inner-diameter line estimated from eqs. (1) and (2) suggesting laminar flow in the viscometer tube. In the present work,  $D = 8.23$  mm and  $\theta = 10^\circ$  ( $d = 8.00$  mm) were selected. These are in the conditions of laminar flow for both H<sub>2</sub>O and D<sub>2</sub>O at all pressures and temperatures where we measured.

Using several solvents whose viscosity values are known as samples, we measured the  $t$  at atmospheric pressure. The results is plotted as a function of  $(\rho_b - \rho)t$  in Fig. 6. Observed linear line which goes through the origin also suggests that eq. (2) is effective for our viscometer to estimate the viscosity even at low values such as heptane [1].

*Evaluation of the Instrument Constant:* Instrument constant,  $K$ , can be calculated by using eq. (2). But its accuracy is not good because  $\theta$  can not be precisely estimated and is changeable at each sample filling. Then we estimated the viscosity as an relative one as shown in eq. (3). In this estimation, we have to consider the thermal expansion and compression of the ball and viscometer tube, that is, temperature and pressure dependences of  $D$  and  $d$  in eq. (2). Further a difference of the component in the glass materials (such as SiO<sub>2</sub>, NaO<sub>2</sub>, etc.) between the ball and viscometer tube also has to be considered though the formal name of both materials are the same Pyrex 7740. It might contribute to the difference,  $D-d$ , in eq.(2). But, as the temperature change in the present work is at most 50 K, the difference of  $K$  in eq. (2) is estimated to be  $(0.02 \pm 0.006)\%$  using the linear expansion coefficient of the glass,  $(325 \pm 5) \times 10^{-8} \text{ K}^{-1}$  [12]. It is negligibly small. On the other hand, as the component dispersion of the compressibility of the glass is estimated to be 5% [12] and the several compression data of the glass are known [13, 14], the instrument constant is estimated to decrease by  $(0.33 \pm 0.15) \%$  at 300

MPa. Then we consider such change of  $K$  value by pressure.

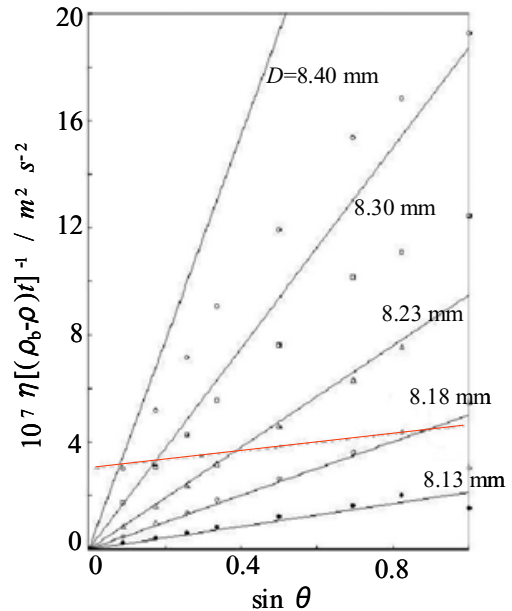


Fig. 5.  $\eta / [(\rho_b - \rho)t]$  vs.  $\sin \theta$  for H<sub>2</sub>O at 298.15 K, 0.10 MPa, and  $d = 8.00$  mm. Dotted line is  $Re_c$  [9].

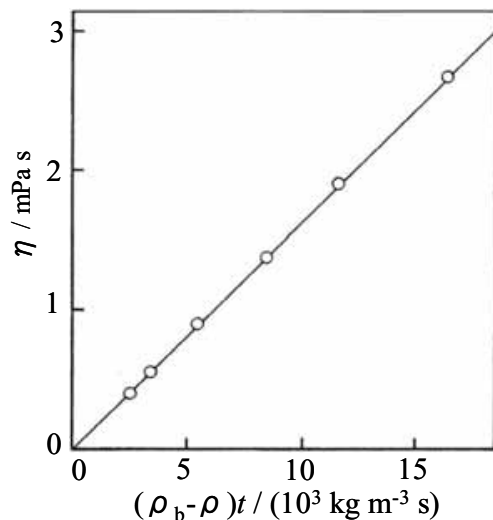


Fig. 6 Relation between  $\eta$  and  $(\rho_b - \rho)t$  for several liquids at 298.15 K and 0.10 MPa. The liquids are heptane, methanol, water, decane, propanol, and butanol in the order of increasing viscosity.

*Density of Sample Liquids* : Density data of H<sub>2</sub>O and D<sub>2</sub>O are required to estimate the viscosity as shown in eq. (1). For H<sub>2</sub>O, a fitting equation of IAPWS [15] (effective at 273.15 - 623 K and vapor pressure - 100 MPa) and Bridgman's data [16] were cited. For D<sub>2</sub>O, IAPWS [17] and Bridgman's [16] were done. Pressure scale by Bridgman [16] was corrected by 1% following the comment by Grindly and Lind [18].

**3.4. Viscosity of H<sub>2</sub>O and D<sub>2</sub>O** Observed viscosity values of H<sub>2</sub>O and D<sub>2</sub>O are shown in Figs. 7 and 8, respectively. Dotted curves in both figures are plotted by using the IAPWS equations [15, 27] though they are effective only in the regions; 273 K <  $T$  < 1173 K and 0.10 MPa <  $p$  < 100 MPa for H<sub>2</sub>O, and 277 K <  $T$  < 775 K and 0.10 MPa <  $p$  < 100 MPa for D<sub>2</sub>O, respectively. Our data for H<sub>2</sub>O does not deviate from IAPWS at the temperature higher than 273 K suggesting an reliability of our measurement. And further the IAPWS curves at lower temperature than 273 K does not so differ from our data. It means that the IAPWS equation will be applicable to this high pressure and low

temperature region without so much modification. On the other hand, the dotted curves of IAPWS for D<sub>2</sub>O do not fit to our data and also to Agayev's [22, 26] in the low temperature and high pressure region which is out of an effective region of IAPWS. Any modification in the fitting curve should be required to use it in the region. We hope that present work contributes to an expansion of the fitting curve to the high pressure and low temperature region.

#### Acknowledgments

Measurement of the roundness of the ball was supported by Industrial Research Center of Shiga Prefecture, Japan.

#### References

- [1] S. Sawamura, N. Takeuchi, K. Kitamura, and Y. Taniguchi, *Rev. Sci. Instr.*, **61**, 871 (1990).
- [2] S. Sawamura, Y. Yoshimura, K. Kitamura, and Y. Taniguchi, *J. Phys. Chem.*, **96**, 5526 (1992).
- [3] Y. Yoshimura, S. Sawamura, Y. Taniguchi, *Z. Naturforsch.*, **50a**, 316 (1995).
- [4] Y. Yoshimura, S. Sawamura, Y. Taniguchi,

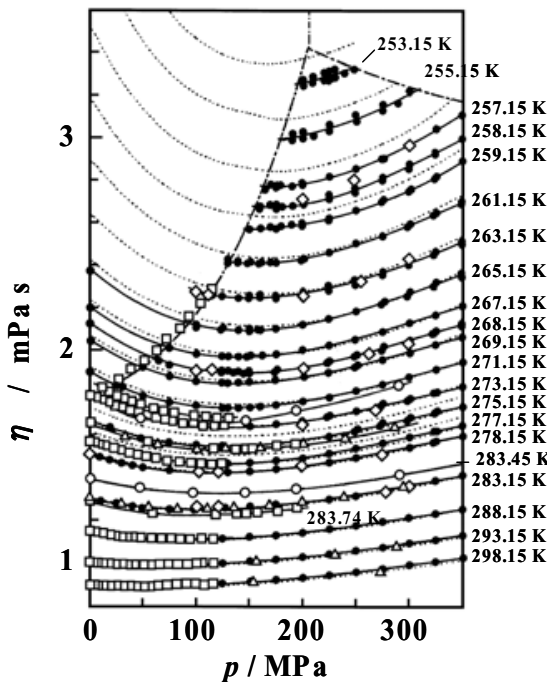


Fig. 7. Viscosity of H<sub>2</sub>O. ●, present work; △, Bridgman [19]; △, Cappi [20]; ◇, DeFries and Jonas [21]; □, Agayev [22,23]; ···, IAPWS [15]

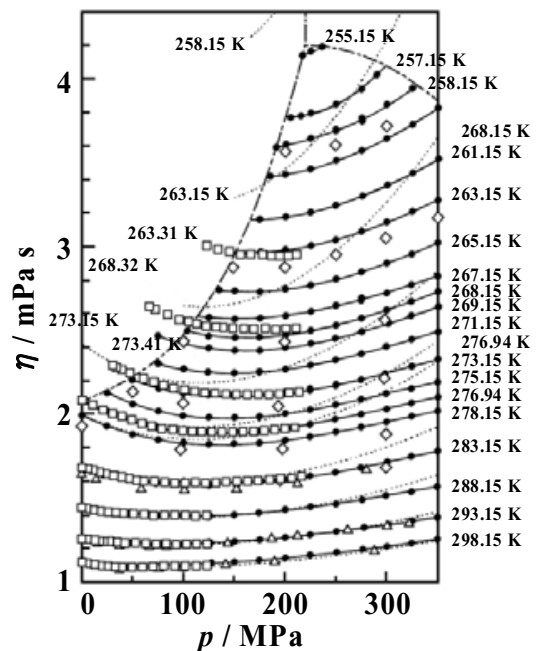


Fig. 8. Viscosity of D<sub>2</sub>O. ●, present work; △, Harlow [24]; ◇, DeFries and Jonas [25], □, Agayev [22,26], ···, IAPWS [27].

- Material Sci. Res. Int.*, **1**, 126 (1995).
- [5] T. Nakai, S. Sawamura, Y. Taniguchi, *J. Mol. Liq.*, **65/66**, 365 (1995).
- [6] T. Nakai, S. Sawamura, Y. Taniguchi, and Y. Yamaura, *Material Sci. Res. Int.*, **2**, 143 (1996).
- [7] T. Nakai, S. Sawamura, Y. Taniguchi, T. Kuboyama, *Material Sci. Res. Int.*, **3**, 204 (1997).
- [8] S. Sawamura, Y. Yoshimura, T. Nakai, Y. Taniguchi, K. Suzuki, *Steam, Water and Hydrothermal Systems: Physics and Chemistry, Proc. 13th Int. Conf. Properties of Water and Steam*, eds. P. Tremaine, P. G. Hill, D. Irish, and P. V. Balakrishnan, NRC Press., Ottawa (2000), p.88.
- [9] R.M.Hubbard and G.G.Brown, *Ind. Eng. Chem., Anal. Ed.*, **15**, 212 (1943).
- [10] H.W.Lewis, *Anal.Chem.*, **25**, 507 (1953).
- [11] Y. Yoshimura, S. Sawamura, J. Matsuda, K. Kitamura, Y. Taniguchi, *J. Soc. Mat. Sci, Japan*, **41**, 318 (1992).
- [12] H. Scholze, *Glass --- Nature, Structure, and Properties*, Springer-Verlag (1991), chap. 3.
- [13] P. W. Bridgman, *Am. J. Sci.*, **10**, 259 (1925).
- [14] L. H. Adams and R. E. Gibson, *J. Wash. Acad. Sci.*, **21**, 381 (1931).
- [15] W. Wagner and A. Kruse, *Properties of Water and Steam*, Springer (1997).
- [16] P. W. Bridgman, *J. Chem. Phys.*, **3**, 597 (1935).
- [17] J. Kestin and J. V. Sengers, *J. Phys. Chem. Ref. Data*, **15**, 305 (1986).
- [18] T. Grindley and J. E. Lind, Jr., *J. Chem. Phys.*, **54**, 3983 (1971).
- [19] P. W. Bridgman, *Proc. Am. Acad. Arts. Sci.*, **61**, 57 (1926).
- [20] J. B. Capii, Ph. D. Thesis, Univ. London (1964).
- [21] T. DeFries, and J. Jonas, *J. Chem. Phys.*, **66**, 896 (1977).
- [22] N. A. Agayev and A. D. Yusibova, *Dokl. Akad. Nauk SSSR, Ser. Mat. Fiz.*, **180**, 334 (1968). [Eng. trans., *Sov. Phys. Dokl.*, **13**, 472 (1968)].
- [23] N. A. Agayev, *Proc. 9th Int. Conf. Properties of Steam 1979*, Pergamon, Oxford (1980), p.362.
- [24] A. Harlow, Ph. D. Thesis, Univ. London (1967).
- [25] T. DeFries and J. Jonas, *J. Chem. Phys.*, **66**, 5393 (1977).
- [26] N. A. Agaev, *Proc. 11th Int. Conf. Properties of Water and Steam 1989*, Prague (1990), p. 148.
- [27] N. Matsunaga and A. Nagashima, *J. Phys. Chem. Ref. Data*, **12**, 933 (1983).